Colloid Polym Sci 278: 1070–1084 (2000)

ORIGINAL CONTRIBUTION

T. Ogasawara
A. Nara
H. Okabayashi
E. Nishio
C. J. O'Connor

Time-resolved near-infrared and two-dimensional near-infrared correlation spectroscopic studies of the polymerization process of silane coupling agents. Dynamic behavior of water molecules in the 3-aminopropyltriethoxysilane–ethanol–water system

Received: 14 March 2000
Accepted: 15 May 2000

T. Ogasawara · H. Okabayashi (✉)
Department of Applied Chemistry
Nagoya Institute of Technology
Gokiso-cho, Showa-ku
Nagoya 466-8555, Japan

A. Nara · E. Nishio
Nicolet Japan, Osaka Laboratory
Terauchi, Toyonaka
Osaka 560-0872, Japan

C. J. O'Connor
Department of Chemistry
The University of Auckland
Private Bag 92019, Auckland
New Zealand

Abstract The polymerization behavior of 3-aminopropyltriethoxysilane, a process initiated by water molecules, has been examined using time-resolved near-IR and 2D near-IR correlation spectra. By deconvolution of the time-resolved near-IR spectra, the existence of the component bands at 5189, 5265 and 5300 cm^{-1}, whose intensities decrease markedly as the reaction proceeds, has been confirmed in the 5000–5400 cm^{-1} region. The band at 5189 cm^{-1} has been assigned to water molecules, while those at 5265 and 5300 cm^{-1} have been assigned to the strongly and weakly associated silanol groups, respectively. The kinetics of the hydrolysis of the ethoxy groups and of the formation of a siloxane bond have been analyzed using the time-dependent integral intensities of these three bands and the mechanisms of the reactions have been discussed. Evidence for this polymerization process is also clearly evident in the 2D near-IR correlation spectra.

Key words Time-resolved near-infrared · Two-dimensional correlation · 3-Aminopropyltriethoxysilane · Condensation

Introduction

The chemical functions of organosilane coupling agents are commonly used to reinforce the mechanical properties of the interface between two different materials, thereby leading to extensive studies of their macroscopic nature [1–3] and molecular structure [4–21] when coated onto the surface of a substrate. One of the most commonly used silanes is 3-aminopropyltriethoxysilane (APTS), which differs from many other organotrialkoxysilanes in that it is very stable, even in aqueous solution. In order to explain this stability, Plueddemann [22] proposed structural models of five- or six-membered rings in which the nitrogen atom of the amino group interacts with either the Si atom or one of the silanol (SiOH) groups. Various structural models of special relevance to this problem have been suggested [9, 23–26].

It is well known that amines form very strong hydrogen bonds with silanols on the surface of a substrate and that the bonded amine renders the Si-O group of the silanol more nucleophilic [27, 28]. Tripp and Hair [29] have proposed a process for face-promoted silanization in a chlorosilane–silica gel system. Thus, the behavior of the NH_2 groups on the surface of a substrate must play a critical role in the process of silanization.

We may speculate that such an interaction between amino and silanol OH groups is possible during the water-initiated polymerization process of APTS in organic solvents, thus affecting the mechanism of the condensation reaction. In the APTS–ethanol–water system, the NH_2, water OH and ethanol OH groups, as well as the silanol OH formed during hydrolysis, should all take part in the interaction through a hydrogen-bonded network [30]. If we could obtain separate information on each of the interactions between NH_2 and water OH or ethanol OH or silanol OH, further detailed discussion of the polymerization process would then be possible. ^1H NMR spectroscopy provides information on the hydrogen-bonding system [31];

however, it is very difficult to observe these interactions separately using ^{1}H NMR spectroscopy, since an exchange reaction exists between the protons.

In this present study, we used 2D near-IR (NIR) correlation spectroscopy to examine the behavior of each of the NH_2, silanol OH, water OH and ethanol OH groups during the polymerization process of APTS initiated by water molecules in ethanol. 2D NIR correlation spectroscopy, which was first proposed by Noda [32–35], is a novel analytical technique, based on time-resolved detection of IR signals, used for elucidating various chemical interactions among functional groups, and its application has been extended to include various areas [36–46].

Experimental

Materials

APTS [$NH_2CH_2CH_2CH_2Si(OC_2H_5)_3$] was purchased from Shinetsu Chemical Industry and was used without further purification. An APTS–ethanol (7:3 w/w) solution was used to follow the condensation reaction between APTS molecules, and a quantity of water, equimolar with that of APTS, was added to initiate the reaction.

Methods

Raman spectra below 4000 cm^{-1} were obtained using a Nicoret 950 Fourier transform Raman spectrometer using the Nd:YAG laser (CVI) excitation wavelength of 1064 cm^{-1} with a resolution of 4 cm^{-1} at room temperature (25 °C). Raman spectra of the sample solution (APTS–ethanol–water) were obtained using a sealed ampoule containing this solution and with a laser power of 400 mW.

Time-resolved IR and NIR spectra of the sample solution sandwiched between two CaF_2 windows using Pb spacers (0.5 mm) were recorded at a resolution of 8 cm^{-1} on a Nicoret Magna System 860 Fourier transform IR spectrometer (800–4000 and 4000–10000 cm^{-1}) equipped with a PTGS KBr detector. The light source used was an He-Ne laser (1579.3 cm^{-1} line). Forty scans were accumulated to ensure an acceptable signal-to-noise ratio.

The technique of Fourier deconvolution was used to resolve superimposed NIR bands. Deconvolution of the bands was made by utilizing the standard Nicolet 1180 software. Gaussian band shapes were assumed for the deconvoluted components.

Synchronous and asynchronous 2D NIR correlation spectral maps were calculated from the time-resolved NIR spectral data using the program 2D-Pocha for generalized 2D correlation spectroscopy.

The method for analysis of a generalized 2D correlation spectrum has previously been described by Noda and coworkers [35, 47] and we briefly describe its background in the following.

A synchronous 2D NIR correlation spectrum provides information on the similarity between the sequential variations of spectral intensities [32–35]. The peaks (autocorrelation peaks or auto-peaks), which are located on the diagonal line, represent the extent of dynamic intensity variation of spectral bands with different wavenumbers. When the spectral coordinates of the cross-peak are observed at two different wavenumbers and the tendency for dynamic variation of their intensities is similar, synchronous cross-peaks then appear at off-diagonal positions. Positive cross-peaks imply that the intensities of the two bands with different wavenumbers are either increasing or decreasing together, while negative cross-peaks (usually shaded) mean that the intensity of one band is increasing while that of the other band is decreasing.

An important characteristic of an asynchronous 2D NIR correlation spectrum consisting only of off-diagonal cross-peaks is the fact that the cross-peaks and their sign directly reflect the difference between the time-dependent sequential variations of NIR band intensities [32, 33, 47, 48]. When the tendency for the variation in intensity of cross-peaks with two different coordinates is for them to be dissimilar to each other, the cross-peaks appear in the asynchronous spectrum. This characteristic is sufficiently powerful to enhance the spectral resolution of highly superimposed NIR bands. It should be emphasized that we can assign the specific sequence for an increase or a decrease in intensity occurring at different times. For example, in the asynchronous spectrum, a shaded cross-peak indicates that the intensity variation (increase or decrease) for the band at wavenumber ν_1 occurs later, compared with that of the band at wavenumber ν_2. An unshaded cross-peak indicates the opposite effect, i.e. the intensity variation occurs sooner.

Results and discussion

Time-resolved Raman scattering and IR spectra

In the APTS–ethanol–water system, the presence of water molecules is one of the most important parameters for initiating the condensation reaction [14, 15], in a manner similar to the role of water during the modification of silica gel with APTS [10, 11, 13]. Water induces hydrolysis of the APTS ethoxy groups (reaction 1), leading to formation of silanol groups which can combine to form a siloxane linkage between two silane molecules, with the release of ethanol and the formation of a new water molecules (reaction 2) [14, 15].

$$H_2NCH_2CH_2CH_2SiL_2(OC_2H_5) + H_2O \rightarrow H_2NCH_2CH_2CH_2SiL_2(OH) + C_2H_5OH \quad (1)$$

$$2H_2NCH_2CH_2CH_2SiL_2(OH) \rightarrow (H_2NCH_2CH_2CH_2)L_2Si\text{-}O\text{-}SiL_2(CH_2CH_2CH_2NH_2) + H_2O \qquad L = \text{-}OC_2H_5, \text{-}OH \text{ or } \text{-}O\text{-}Si \quad (2)$$

During this polymerization process, the release of ethanol induced by water molecules can be easily followed by the use of time-resolved Raman scattering and IR absorption spectra, since the characteristic Raman (IR) spectral bands of ethanol disappear in the reaction spectra of APTS, as discussed later.

In this study, time-resolved Raman scattering (in the 200–4000 cm^{-1} region) and IR spectra (in the 800–4000 cm^{-1} region) of the APTS–ethanol–water system were examined prior to measurement in the near IR. Some of the Raman spectra, time-resolved in the 200–4000 cm^{-1} region, are shown in Fig. 1. The intensities of the characteristic 883 and 1053 cm^{-1} bands of ethanol increase markedly as the reaction proceeds, indicating that ethanol is released.

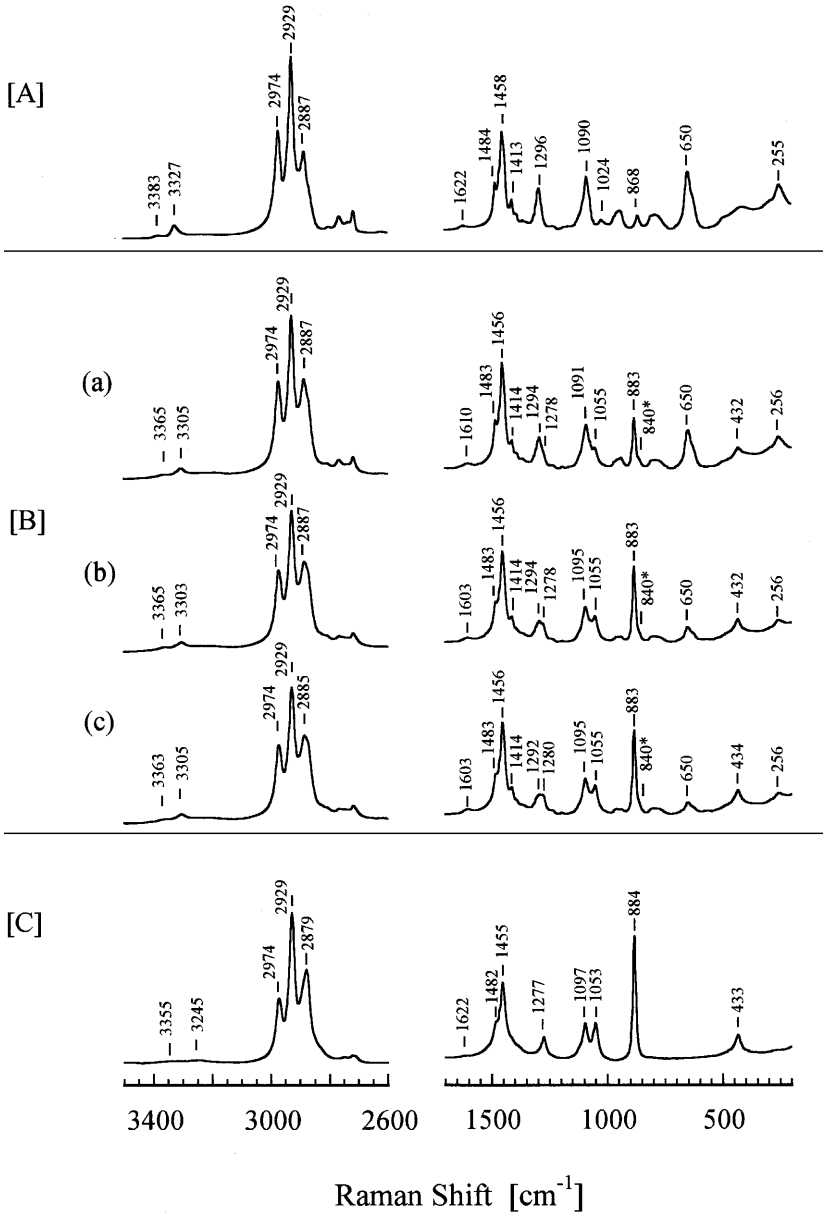

Fig. 1 Raman spectra **A** of liquid 3-aminopropyltriethoxysilane (*APTS*), **B** of the APTS–ethanol–water system at reaction times 60 s (*a*), 9240 s (*b*) and 16500 s (*c*) and **C** of ethanol. The Raman band at 840 cm^{-1} (marked with an *asterisk*) is tentatively assigned to the SiOH bend mode

The relative intensity, I_{883}/I_{1456}, of each of the time-resolved Raman spectra was calculated. The 1456 cm^{-1} band, arising from the CH_3 and CH_2 deformation modes of the propyl segment, the three ethoxy groups and ethanol, was selected as a reference.

In order to interpret these time-dependent Raman scattering data, it is necessary to invoke a relatively fast initial reaction process, followed by at least one slower process, since the time dependence of the concentration of released ethanol cannot be expressed by a single exponential function. We analyzed the time-dependent data of the APTS reaction mixture and found that two sequential first-order reaction processes (initial and second rate constants, k_i and k_s, respectively) participate in the overall reaction and that these can be separated from the overall reaction process. The data analysis was carried out as follows.

We can express the two reaction processes by reactions 3 and 4, neglecting the reverse reactions.

$$M \xrightarrow{k_i} E_i + P_1 \tag{3}$$

$$P_1 \xrightarrow{k_s} E_s + P_2 \tag{4}$$

In the initial reaction, hydrolysis of APTS monomers (M) brings about formation of P_1 with unreacted ethoxy groups and release of ethanol (E_i). In the second reaction, hydrolysis of species P_1 leads to further release

of ethanol (E_s) and then production of the P_2 species with fewer unreacted ethoxy groups than exist in P_1.

Two molecules of ethanol are released from the condensation reaction between one APTS molecule and one water molecule; therefore, when water molecules, equimolar with the initial concentration of APTS, are added to the APTS–ethanol (7:3 w/w) solution, two of the three ethoxy groups of APTS are hydrolyzed and two molecules of ethanol are released.

The time dependence of the concentration c^M, c^E_{obs} and c^{P_1} are as follows:

$$c^M = c^E_\infty e^{-k_i t} \tag{5}$$

$$c^E_{obs}(t) = c^{E_i}(t) + c^{E_s}(t) \tag{6}$$

$$c^{E_i} = c^E_\infty (1 - e^{-k_i t}) \tag{7}$$

$$c^{E_s} = -\frac{c^E_\infty}{k_s - k_i}(k_s e^{-k_i t} - k_i e^{-k_s t}) + c^E_\infty \tag{8}$$

$$c^{P_1} = \frac{k_i}{k_s - k_i} c^E_\infty (e^{-k_i t} - e^{-k_s t}) \ , \tag{9}$$

where $c^{M_0} = c^E_\infty$.

The kinetics of the time-dependent Raman data may therefore be analyzed using only two parameters (k_i and k_s); thus, kinetics analysis could be made for all relative intensity data (I_{883}/I_{1456}).

Plots of $c^E_{obs}(t)$ versus t, which provide the best fit of the calculated values to the observed data at 298 K, are shown in Fig. 2 together with plots for separated curves

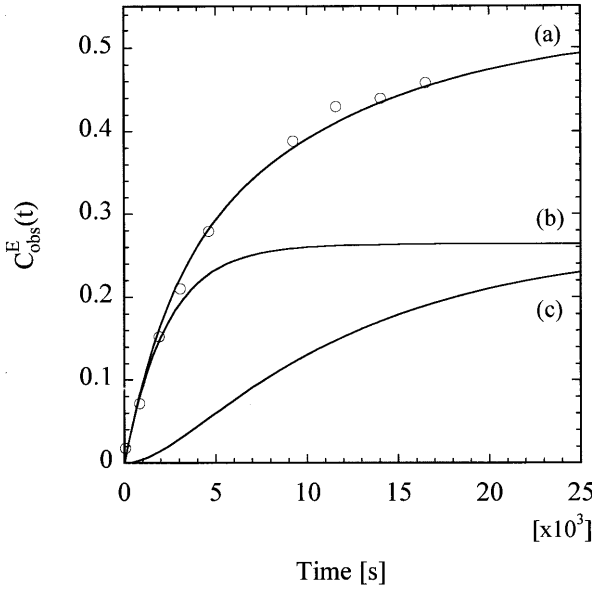

Fig. 2 Plots of $c^E_{obs}(t)$ against t (○: observed) and best-fit curves (*solid lines*) for the APTS–ethanol–water system. Curves *b* and *c* are the initial and second reaction process curves separated from the best-fit curve (*a*)

Table 1 Rate constants for initial and second reactions as obtained from Raman and near-IR (*NIR*) spectra

Hydrolysis			
Ethanol release (I_{883}/I_{1456})	(Raman)	k_i (s^{-1}) 4.31×10^{-4}	k_s (s^{-1}) 9.18×10^{-5}
Water consumption [$(\nu_2 + \nu_3)$band]	(NIR)	k_i^w (s^{-1}) 2.98×10^{-4}	k_s^w (s^{-1}) 7.45×10^{-5}
Condensation			
Weakly associated SiOH (5300 cm^{-1})	(NIR)	k_i^c (s^{-1}) 2.99×10^{-4}	k_s^c (s^{-1}) 5.56×10^{-5}
Strongly associated SiOH (5265 cm^{-1})	(NIR)	k_i^c (s^{-1}) 3.55×10^{-4}	k_s^c (s^{-1}) –

of the initial and second reactions. Values of k_i and k_s, as obtained from the plots, are given in Table 1.

Time-resolved IR spectra in the 800–4000 cm^{-1} region were also examined. The 882 and 1050 cm^{-1} bands, characteristic of ethanol, increase in absorbance with time and can be used as a probe for ethanol release (Fig. 3). However, in this study, only Raman scattering data were used in the calculations.

Stretch and bend modes of the -OH and -NH_2 groups

Raman and IR spectra of the APTS–ethanol–water system below 4000 cm^{-1} are sufficiently resolved to follow the ethanol-release process in the APTS–ethanol–water system. However, it is very difficult to use the Raman and IR spectra in this region, to study independently the behavior of each of the silanol OH, ethanol OH, water OH and APTS NH_2 groups during the polymerization process, since the vibrational bands coming from the stretch and bend modes of the OH and NH_2 groups are superimposed upon each other in the 3000–4000 and 1500–1700 cm^{-1} regions. Moreover, their bands are both very broad and very weak.

In the near IR spectrum of the APTS–ethanol–water system, the overtones of the stretch modes of the OH and NH_2 groups, in addition to those of the CH stretch modes of the CH_2 and CH_3 groups, and the combination bands between the stretch and bend modes, are usually predominant. Moreover, the bands characteristics of silanol OH, as well as those characteristic of the water OH, ethanol OH and NH_2 groups, should be observed separately. In order to interpret the NIR bands of the APTS–ethanol–water system, interpretation of the Raman (IR) bands coming from the stretch and bend modes of the OH and NH_2 groups must be clarified. The wavenumbers of these bands are summarized in Table 2 together with those of trimethylchlorosilane (TMCS) [5] and APTS in the liquid state (spectra not shown). Since assignment of the stretch and bend modes of the water OH and ethanol OH groups has already been elucidated

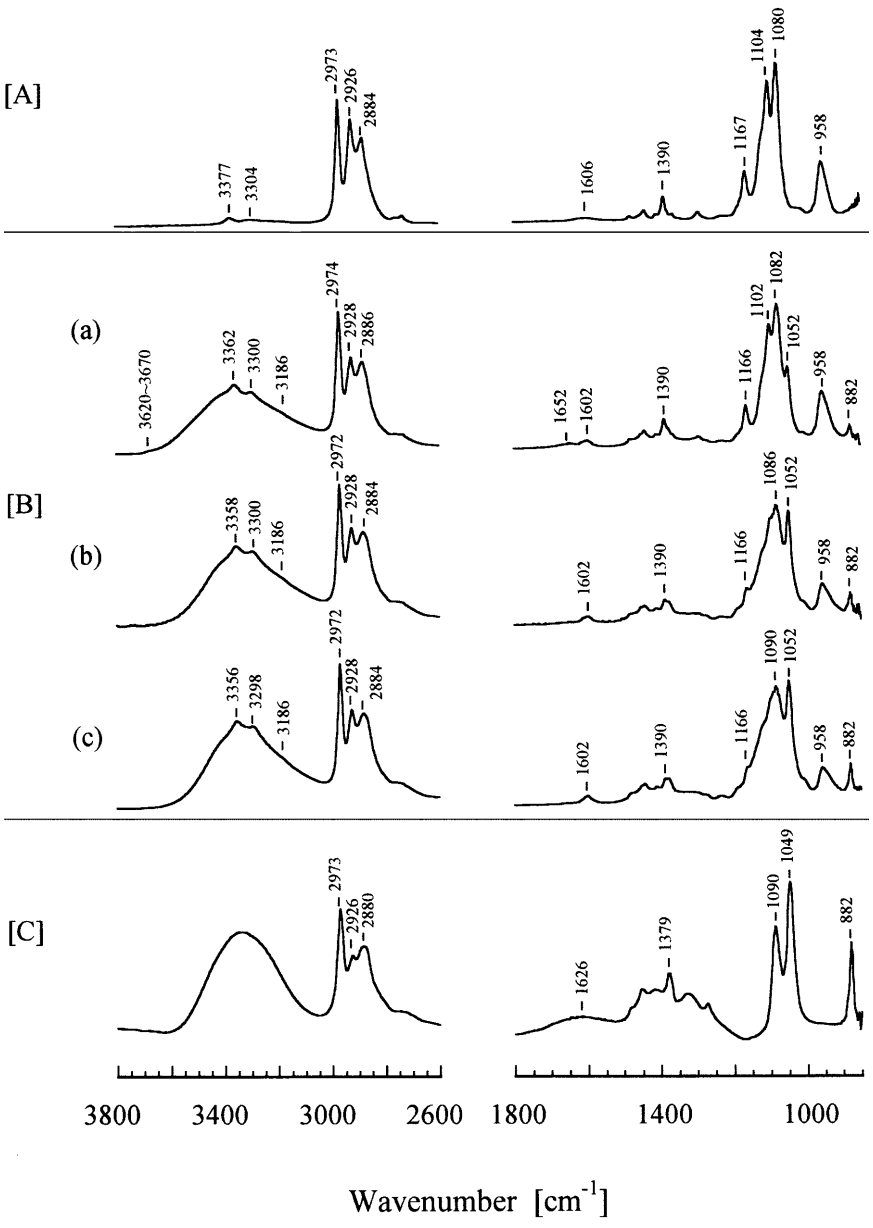

Fig. 3 IR spectra **A** of liquid APTS, **B** of the APTS–ethanol–water system at reaction time 60 s (*a*), 9240 s (*b*) and 16500 s (*c*) and **C** of ethanol

[49]. In this study, we mainly describe the OH stretch and bend modes of the silanol group, which plays an important role in the reaction, and those of the NH_2 groups, which are sensitive to the $NH_2 \cdots OH$ interaction.

As shown in Fig. 3, an extremely weak and broad IR band at 3620–3670 cm^{-1} is found in the APTS–ethanol–water system. This band appears in the initial stage of the reaction and its absorbance gradually decreases with time, until the band essentially disappears. We may assign this band to the OH stretch modes of the SiOH groups which are produced by hydrolysis [14, 15] and which, judging from the data in previous studies [13, 14], participate in the associated system through hydrogen bonds with the water OH, ethanol OH and NH_2 groups. Therefore, the band at 3620–3670 cm^{-1} should be regarded as a superimposition of at least two bands, which come from the OH stretch modes of weakly and strongly associated SiOH systems.

Shih and Koenig [5] examined the Raman scattering of TMCS before and after its hydrolysis and found Raman bands at 3625 and 3702 cm^{-1} for the hydrolyzed sample, which were assigned by Batuev et al. [6] to the vibrations of unassociated and associated SiOH groups, respectively. They also found Raman bands at 834 and 880 cm^{-1} and assigned the 880 cm^{-1} band to the bending mode of the SiOH group. Although they did not assign the 834 cm^{-1} band, it probably comes from

Table 2 Combination and overtone bands expected from the stretch (ν) and bend (δ) modes of silanol OH and NH_2 groups

	Observed OH band (cm^{-1})		Combination ($\nu + 2\delta$) (cm^{-1})		Overtone (2ν) (cm^{-1})	
	ν (OH)	δ (SiOH)	Expected	Observed	Expected	Observed
SiOH						
	(Raman)	(Raman)	NIR		NIR	
Trimethylchlorosilane [5]	3702	880	5432	–	7404	–
	3625	834	5293	–	7250	–
	(IR)	(Raman)	NIR		NIR	
3-Aminopropyltriehoxylsilane–ethanol–H_2O	3620–3670	830–880	5300–5430	5300 (5265)[a]	7240–7340	7200–7350
	Observed (cm^{-1})		Combination ($\nu + \delta$) (cm^{-1})		Overtone (2ν) (cm^{-1})	
	Stretch (ν)	Bend (δ)	Expected	Observed	Expected	Observed
NH_2						
	IR		NIR		NIR	
	3377 (ν_{asy})	1622				
3-Aminopropyltriethoxysilane (liquid)	3304 (ν_{sym})	1575	4999	5009	6754	6716
		1545	4952	4943	6608	6539
	IR		NIR		NIR	
	3356–3362 (ν_{asy})	1602	4958–4964	4958	6712–6724	6695
3-Aminopropyltrimethoxysilane–ethanol–H_2O	3300(ν_{sym})	1575	4931–4937	4925	6600	6540
	3186 (NH···OH)		4731	4721	6372	6483

[a] This band was confirmed in the deconvoluted spectra (Fig. 6)

the bending mode of the associated SiOH groups. Benesi and Jones [7] found a 870 cm^{-1} band in the IR spectrum of silica gel and assigned it to the same mode. Richards and Thompson [8] found a strong IR band in the 830–880 cm^{-1} region arising from the silanol groups on the silica surface. Thus, we may assume that the associated SiOH groups provide the bending modes, in the 830–880 cm^{-1} region, whose wavenumber strongly depends upon the strength of the hydrogen bonds.

In the APTS–ethanol–water system, the presence of the NH_2 groups in an APTS molecule makes it possible for silanols to participate in inter- and intramolecular $SiOH\cdots NH_2$ type hydrogen-bonding, leading to a downward shift in the SiOH bending mode. Thus, in the Raman spectra of the APTS–ethanol–water system, shoulder bands at 840 cm^{-1} may be assigned to the bending modes of the associated SiOH groups and the 883 cm^{-1} bands may be due to superimposition of the bending mode of the weakly associated SiOH group upon the 880 cm^{-1} band characteristic of released ethanol (Table 2). The existence of unassociated and associated silanol groups should bring about the appearance of two combination [$\nu_{SiOH}(OH) + 2\delta(SiOH)$] bands in the 5000–5400 cm^{-1} region (discussed later).

In a previous study [31], we examined the IR spectra of APTS–toluene solutions at various concentrations and showed that the spectral features of the asymmetric [$\nu_{asy}(NH_2)$] and symmetric [$\nu_{sym}(NH_2)$] stretch modes of the NH_2 group are dependent on concentration. In dilute solution, these bands appeared at 3840 and 3324 cm^{-1}, wavenumbers very close to the 3392 and 3352 cm^{-1} bands, respectively, of typical straight-chain amines [30]. They may, therefore, be assigned to the ν_{asy} and ν_{sym} modes of unassociated NH_2 groups or to the NH_2 groups which participate in a very weak hydrogen-bonding system. At higher APTS concentration, it was found that a shoulder band at around 3300 cm^{-1} appears beside the 3324 cm^{-1} band and that its intensity increases with increasing concentration until the spectral feature approaches that of APTS in the liquid state (ν_{asy}: 3377 cm^{-1}, ν_{sym}: 3304 cm^{-1}). Therefore, we may assume that such concentration dependence of the $\nu_{asy}(NH_2)$ and $\nu_{sym}(NH_2)$ modes arises from hydrogen-bond formation between the NH_2 groups in the APTS aggregates. For APTS molecules in the liquid state, most of the silane molecules probably form aggregates held together by a network of hydrogen bonds.

Thus, the bands at 3298–3300 and 3356–3362 cm^{-1} observed in the APTS–ethanol–water system may come from the network of relatively strong hydrogen bonds formed between the NH_2 groups in the aggregates. The shoulder bands at 3186 cm^{-1} should be ascribed to the NH_2 stretch modes participating in the stronger hydrogen-bonding system.

Formation of the network of hydrogen bonds affects the wavenumber of the NH_2 bend [$\delta(NH_2)$] modes.

Morimoto et al. [30] found that liquid *n*-butylamine exhibits an IR band at 1605 cm^{-1}, which is assigned to the $\delta(NH_2)$ mode, and that the band shifts to 1580 cm^{-1} in $CHCl_3$. In the diffuse reflectance Fourier transform spectra of the APTS-modified silica gel samples [19], shoulder bands at 1545 and 1570–1580 cm^{-1} were observed and were assigned to the δ modes of the NH_2 groups which participate in a stronger hydrogen-bonding system, i.e. to different $NH_2\cdots OH$ interaction modes. Consequently, we may expect that these modes, which provide different wavenumbers for the NH_2 stretch and bend modes, reflect a corresponding region in the NIR spectrum.

In this study, shoulder bands at 1540–1545, 1560 and 1575 cm^{-1} were also observed in the expanded IR spectrum of the APTS–ethanol–water system and in that of liquid APTS (spectra not shown).

Time-resolved NIR spectra of the polymerization process

In order to examine separately the behavior of water molecules and of the ethanol released in the polymerization process, time-resolved NIR spectra of the APTS–ethanol–water system were measured in the 4000–10000 cm^{-1} region. Of the 800 time-resolved NIR spectra observed, 20 time-resolved spectra (in particular, those in the 4000–7500 cm^{-1} region) are shown in Fig. 4.

Most of the NIR bands in the 4000–4600 cm^{-1} region mainly reflect the combination $[\nu(CH) + \delta(CH_2)]$ modes between the CH_3 or CH_2 stretch $[\nu(CH)]$ and bend $[\delta(CH_2)]$ modes. Therefore, in the NIR spectra of the APTS–ethanol–water system, a $(CH_2)_3$ group of the aminopropyl segment and three CH_3CH_2O groups and ethanol contribute to the NIR bands in this region. Since the condensation reaction brings about the time-dependent release of ethanol, in the time-resolved NIR spectra the bands coming from ethanol tend to increase in intensity, as seen in Fig. 4. We note that the combination $[\nu_{SiOH}(OH) + \delta(SiOH)]$ modes of an OH stretch $[\nu_{SiOH}(OH)]$ and the deformation $[\delta(SiOH)]$ modes of an SiOH group appear in this region. Wood et al. [50] assigned the NIR bands at 4348, 4444 and 4545 cm^{-1} for silica gel to the combination $[\nu_{SiOH}(OH) + \delta(SiOH)]$ modes coming from the hydrogen-bonded cluster, isolated hydrogen-bonded and vicinal hydrogen-bonded SiOH groups, respectively, and Nogami and Morita [51] reported the appearance of a band at 4527 cm^{-1} arising from the SiOH group in the NIR spectra of silica gel. Accordingly, the $[\nu(CH) + \delta(CH_2)]$ modes of the propyl segment and the $[\nu_{SiOH}(OH) + \delta(SiOH)]$ modes of the SiOH groups are superimposed in this region.

The NIR spectra in the 4600–4900 cm^{-1} region may reflect the combination modes between the stretch and deformation modes of the NH_2 groups, whose wavenumber depends markedly upon the strength of the hydrogen bonds, as discussed previously. Therefore, combinations between the 3186 and 1545 or 1575 cm^{-1} bands and between the 3300 and 1545 or 1575 cm^{-1} bands may provide the 4721 and 4837 cm^{-1} bands in the NIR spectrum. Furthermore, in the NIR spectrum of ethanol, a broad 4802 cm^{-1} band appears, which comes from the combination band between the ethanol OH

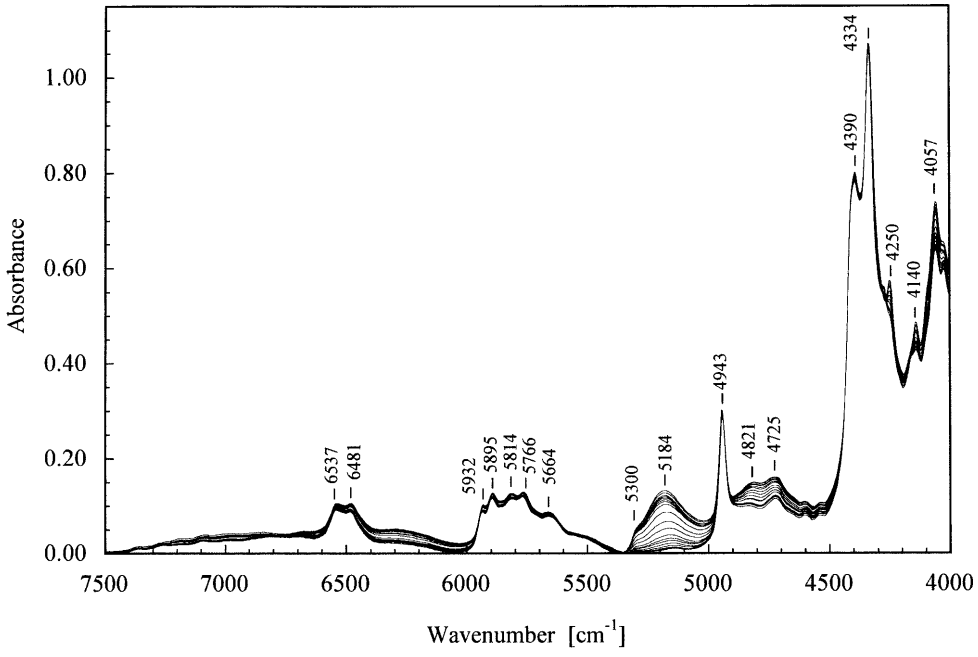

Fig. 4 Time-resolved near-IR (*NIR*) spectra in the 4000–7500 cm^{-1} region for the APTS–ethanol–water system. (Of the 800 NIR spectra obtained, only the 20 spectra collected in the time interval 1. 357 (top of spectrum)–359.070 (bottom of spectrum) min are shown.)

stretch and bend modes; therefore, the ethanol 4802 cm^{-1} band, which is produced as a consequence of the polymerization and whose intensity increases as the reaction proceeds, predominantly contributes to the NIR spectrum in the 4600–4900 cm^{-1} region.

As seen in Fig. 4, in the time-resolved NIR spectra for the APTS–ethanol–water system, it is evident that, as the reaction proceeds, a marked increase in absorbance occurs in this region. In particular, we note that the 4837 cm^{-1} bands shifts downwards markedly with reaction time (to 4810 cm^{-1} after 24 h) and simultaneously absorbance of this band increases, showing that the contribution of the 4802 cm^{-1} band, following release of ethanol, becomes greater with reaction time; however, no downward shift of the 4721 cm^{-1} band occurs, although its absorbance increases markedly with time. This observation is probably due to an increase in the hydrogen-bonding interaction between the NH_2 groups and the ethanol OH groups. Thus, the NIR spectra in the 4600–4900 cm^{-1} region evidently reflect the interaction through hydrogen bonding between the NH_2 and OH groups.

In the time-resolved NIR spectra, the 4945 cm^{-1} band, whose feature is apparently almost independent of reaction time, may be assigned to the combination ($\nu_{asy} + \delta$) bands between the NH_2 asymmetric stretch bands (ν_{asy}: 3362–3356 cm^{-1}) and the NH_2 bend bands (1610–1602 cm^{-1}).

The time-resolved NIR bands at 5184 cm^{-1} come mainly from water molecules and are assigned to the combination ($\nu_2 + \nu_3$) modes between the H_2O deformation (ν_2) and H_2O asymmetric stretch (ν_3) modes [49]. The bands in the 6800–6900 cm^{-1} region may be assigned to the combination mode ($\nu_1 + \nu_3$) between an H_2O symmetric stretch mode (ν_1) and a ν_3 mode.

We note that the combination bands at 5184 cm^{-1} strongly depend upon reaction time. The 3D time-resolved NIR spectra in this region are shown in Fig. 5. Deconvolution of the time-resolved NIR spectra was carried out and the deconvoluted component bands at 5189, 5265 and 5300 cm^{-1} were confirmed in the 5000–5400 cm^{-1} region (discussed later). It is evident that the ($\nu_2 + \nu_3$) band at 5189 cm^{-1} decreases in absorbance with reaction time, indicating that water molecules are consumed in the polymerization process and that the time dependence of the area (integral intensity) of the 5189 cm^{-1} band reflects the rate of this reaction (i.e. of hydrolysis). The time dependence of the relative integral intensity of the 5189 cm^{-1} band is shown in Fig. 6 together with those of the 5265 and 5300 cm^{-1} bands.

In particular, in addition to the time dependence of the 5189 cm^{-1} band, it should be emphasized that the bands at 5265 and 5300 cm^{-1} tend to decrease in intensity and depend upon reaction time.

The 5265 and 5300 cm^{-1} bands may come from the strongly associated and weakly associated silanol groups, respectively, and may be assigned to the combination [ν_{SiOH}(OH) + 2δ(SiOH)] modes (5300 cm^{-1}) between the ν_{SiOH}(OH) modes (3620–3670 cm^{-1}) and the overtone (2δ) of the δ(SiOH) modes (830–840 cm^{-1}) (Table 2); therefore, the time-dependent integral intensities of the bands at 5265 and 5300 cm^{-1} obviously reflect the kinetics of the condensation reaction between the SiOH groups, as discussed later.

Nishio et al. [52] examined a silane layer coated onto the surface of a glass internal reflection element using Fourier transform NIR attenuated total reflectance spectroscopy. They should that the 5140 cm^{-1} band

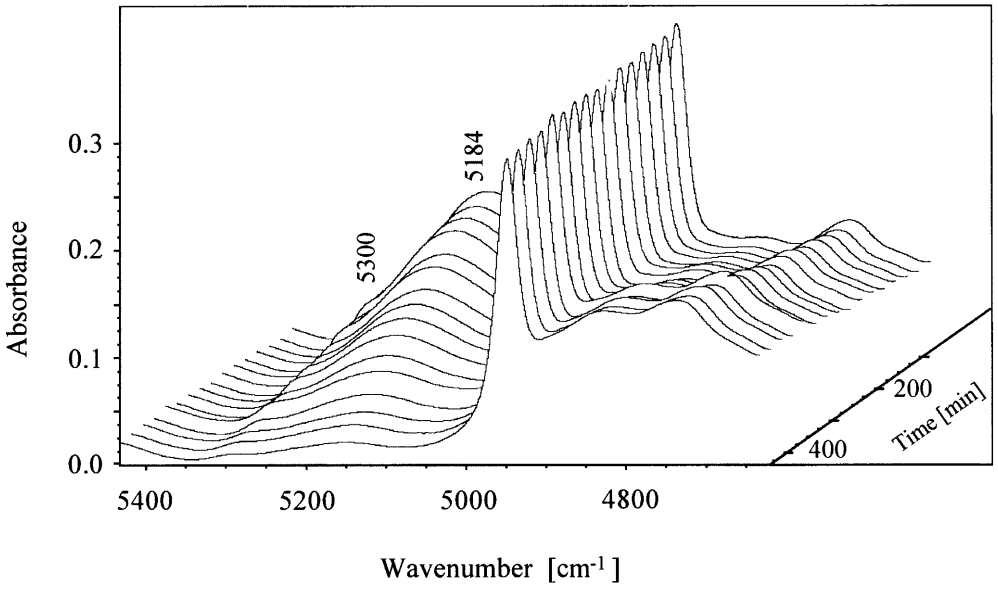

Fig. 5 3D NIR spectra of the APTS–ethanol–water system extended to the 4600–5400 cm^{-1} region

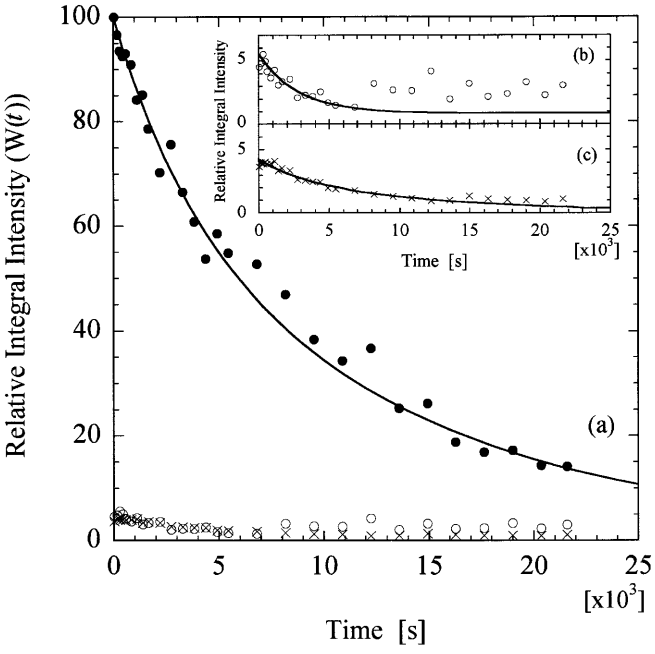

Fig. 6 Time-dependence of relative integral intensities for the bands of water ($v_2 + v_3$) (*a*), and at 5265 cm^{-1} (○, *b*) and 5300 cm^{-1} (×, *c*). The *insets* are the extended expressions of the 5265 and 5300 cm^{-1} bands

comes from the silanols and is superimposed upon the ($v_2 + v_3$) band of water.

In the 6000–6400 cm^{-1} spectral region, an increase in absorbance is also found as the reaction proceeds. This increase may be caused by an increase in the amount of ethanol released by the reaction, since the NIR spectrum of ethanol provides the broad band seen at around 6300 cm^{-1}.

The NIR bands at 6483 and 6538 cm^{-1} may be assigned to the overtones of the asymmetric [$v_{asy}(NH_2)$] and symmetric [$v_{sym}(NH_2)$] stretch modes of the NH_2 groups which participate in the hydrogen-bonding system and which were observed at around 3300 and 3360 cm^{-1}. The reaction induces a slight increase in absorbance for these overtone bands, probably reflecting the environmental variation induced by the release of ethanol around the NH_2 groups through hydrogen bonding.

Kinetics of hydrolysis and condensation reactions

We attempted to deconvolute these time-resolved NIR spectra, using Wilson and Miller's method [50], in order to investigate the kinetics of the hydrolysis and condensation reactions. The time slices of deconvoluted spectra are shown in Fig. 7. Four components (5300, 5265, 5189 and 5080 cm^{-1}) were confirmed in the region 5000–5400 cm^{-1}. The 5300 and 5265 cm^{-1} bands may be assigned to the [$v_{SiOH}(OH) + 2\delta(SiOH)$] modes of weakly and strongly associated SiOH systems, respectively, (Table 2) and, in particular, their intensity depends upon reaction time. The band at 5189 cm^{-1}, which is assigned to the ($v_2 + v_3$) mode of an H_2O molecule, is time-dependent in both wavenumber and intensity. The 5080 cm^{-1} band can be possibly assigned to the ($v_2 + v_3$) modes of tightly hydrogen bonded H_2O molecules in the system. Thus, it is evident that the bands at 5300 and 5265 cm^{-1} reflect the kinetics of the condensation reaction between silanol groups and the band at 5189 cm^{-1} reflects the kinetics of the hydrolysis reaction for ethoxy groups.

For the time-resolved integral intensity data of the 5189 cm^{-1} component band, the kinetics was analyzed using the two-reaction process model which was used for kinetics analysis of the process for release of ethanol. That is, in the initial step, water molecules are consumed during the hydrolysis of the APTS molecules which accompanies the release of ethanol (E_i), and a chemical species (P_1) with many unreacted ethoxy groups is formed. In the second step, water molecules are further utilized for hydrolysis of the species P_1 and further ethanol (E_s) is then released, with production of the P_2 species.

Analysis of the kinetics was carried out as follows. Of the integral intensity data obtained for the 5189 cm^{-1} component band, the initial three data were utilized to obtain the integral intensity value, $W(t)$, at $t = 0$ in a plot of $W(t)$ against t. Using a linear approximation, therefore, the time dependence of the water concentrations, $c(t)$, can be expressed as follows.

$$c(t) = W(0) - W(t) \tag{10}$$

Figure 8 shows plots of $W(t)$ versus t, for the 5189 cm^{-1} band, which give the best fit of the calculated values to the deconvoluted data (at room temperature, around 25 °C) together with plots for the separated curves of the initial and second steps. $W(t)$ at $t = 0$ was made equal to 100; therefore, all the $W(t)$ values are expressed by the relative integral intensity. Values of the hydrolysis reaction rate constants (k_i^w and k_s^w, respectively) in the initial and second steps, thus obtained, are given in Table 1. It is found that the k_i^w and k_s^w values approximately correspond to the k_i and k_s values ($k_i = 2.77 \times 10^{-4}\ s^{-1}$ and $k_s = 0.733 \times 10^{-4}\ s^{-1}$) for the reaction involving release of ethanol which were obtained using the ^1H NMR method in a previous study [54].

For the component band at 5300 cm^{-1}, similar analyses were made, assuming the two-step model. Values of the condensation reaction rate constants (k_i^c and k_s^c) in the initial and second steps are also given in Table 1. For the 5269 cm^{-1} band, the exponential curve (Fig. 6), which was best fitted to the relative integral intensities of the bands obtained in the time range

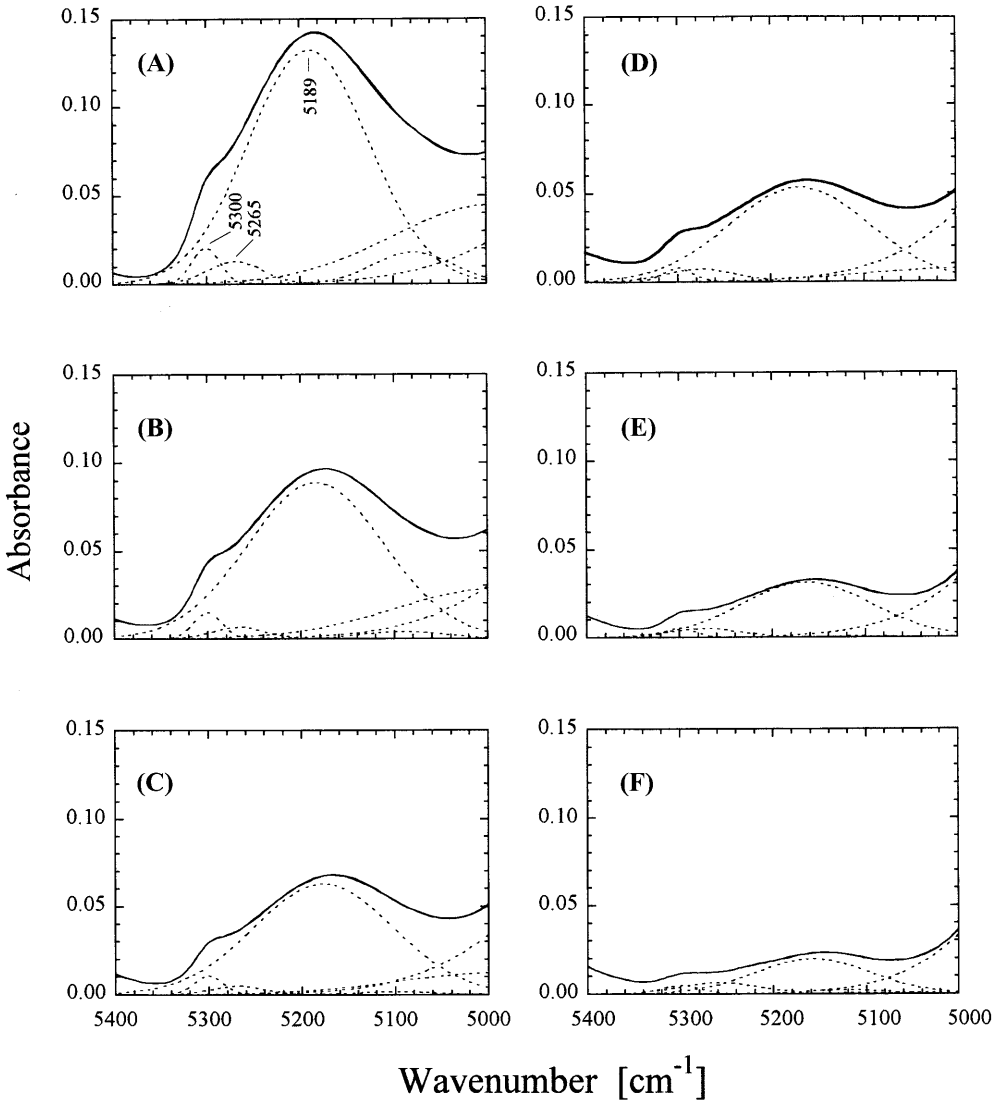

Fig. 7 Time slices (**A** 30 s, **B** 2740 s, **C** 5450 s, **D** 8162 s, **E** 13580 s, **F** 21600 s) of the NIR spectra of the APTS–ethanol–water system and their deconvolutions

0–7000 s since the bands obtained at $t > 7000$ s were too weak in intensity to regard as time-dependent data for the kinetics analysis, was utilized to calculate the rate constant (k_1^c). The result of the kinetics analysis for the 5265 cm^{-1} band may indicate that the consumption of the strongly associated silanols occurs in a single step and that most of this reaction is complete in the initial step, even if the intensity data at $t > 7000$ s are not taken into account for the analysis since the exponential curve for the 5265 cm^{-1} band, obtained at $t < 7000$ s, decreases more steeply than that for the 5300 cm^{-1} band.

Time dependence of the hydrogen-bonding environment of water molecules

The time dependences of the wavenumbers of the observed combination band ($\nu_2 + \nu_3$) (5184 cm^{-1}) and the deconvoluted component band (5189 cm^{-1}) are shown in Fig. 9. Evidently, the wavenumbers of these bands shift rapidly downwards with reaction time, indicating that the reaction induces variation in the hydrogen-bonding environment of the water molecules. In particular, we note that plots of wavenumber versus t consist mainly of two linear portions with different slopes. We may assume for the observed (5184 cm^{-1}) bands that the initial reaction induces a rapid downward shift of the ($\nu_2 + \nu_3$) band until the extent of the downward shift becomes slower at around 8000 s (about 2 h) and finally stops at around 24800 s (about 7 h), showing that consumption of the water molecules which induces the reaction is virtually complete at this time. Similar time dependence was also found for the component band (5189 cm^{-1}) in the deconvoluted spectra (Fig. 9 curve b). This result reveals that during the polymerization process the hydrogen-bonding environ-

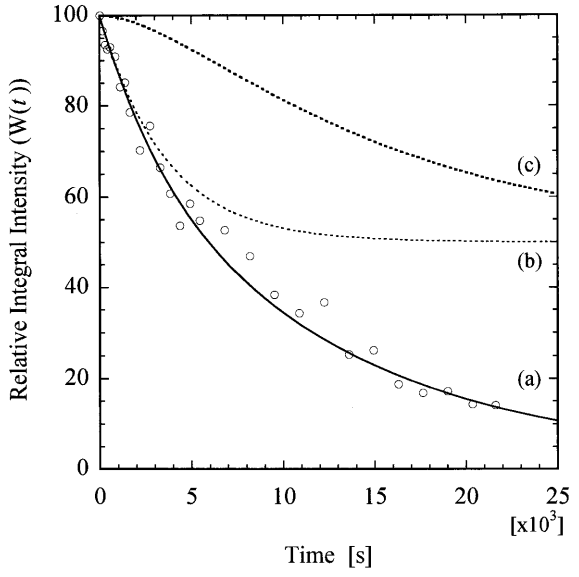

Fig. 8 Plots of relative integral intensity $W(t)$ against t (○: observed) and best-fit curves (*dotted lines*) for the APTS–ethanol–water system [$W(t)$ at $t = 0$ for the 5189 cm^{-1} band was made to equal 100]. Curves *b* and *c* are the initial and second reaction process curves separated from the best-fit curve (*a*)

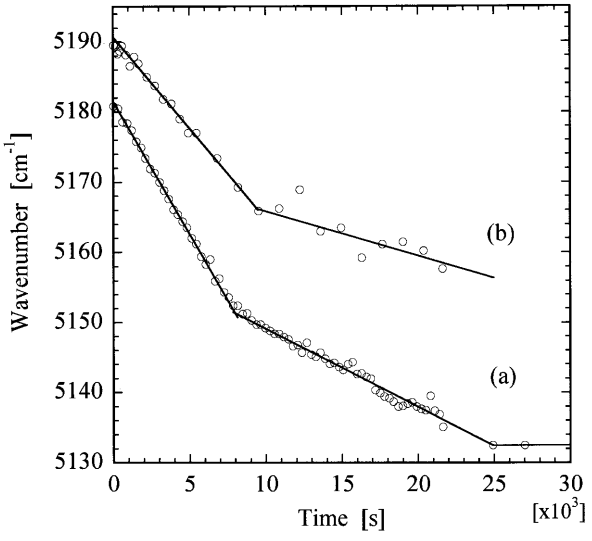

Fig. 9 Time dependence of the wavenumber of the water ($\nu_2 + \nu_3$) band (5184 cm^{-1}) (*a*) and the component band (5189 cm^{-1}) (*b*)

ment of the water molecules changes in a two-step process, which consists of an initial step (about 2 h) and a later step.

In a previous article [53], we presented a time-resolved small-angle X-ray scattering study of the acid-catalyzed condensation reaction of *n*-alkylalkoxide. The time dependence of the apparent radius of gyration, obtained from the Guinier plots, showed that the growth of the polymeric precursors occurs in a two-step process, in which small oligomeric clusters are formed in the initial step and the formation of larger polymeric clusters occurs in the second step. Thus, we may expect the condensation reaction of APTS to occur in a similar two-step process. Accordingly, we may assume that the initial downward shift comes from formation of hydrogen bonding between small oligomeric precursors and water molecules and that the second downward shift is due to the formation of hydrogen bonds between polymeric precursors and water molecules, i.e. the size of the hydrogen-bonding network and the strength of the hydrogen bonds may be different between the initial step and the second step in the present reaction system. The extent of branching (the number of aminopropyl segments) in a small oligomeric precursor should be less than that in a larger polymeric precursor, leading to a difference in the size of the network and in the strength of the hydrogen bonds between a small oligomer and a larger polymeric molecule and to a variation in the wavenumber of the ($\nu_2 + \nu_3$) combination mode in a two-step process.

2D NIR correlation spectra of the APTS–ethanol–water system

The 2D NIR correlation spectra of the APTS–ethanol–water system are shown in Figs. 10 and 11. In the synchronous correlation spectrum (Fig. 10A; synchronous map A), which was calculated from the NIR spectra time-resolved for the first 2 h of reaction, an autocorrelation peak (always positive) at the diagonal position of the coordinate (5200, 5200) and two negative cross-peaks at coordinates (4800, 5200) and (5200, 4800) are found. The synchronous spectrum (Fig. 10B, synchronous map B), which was calculated from the NIR spectra time-resolved for the later 6 h, provides almost the same pattern as that calculated from the initial 2 h time-resolved NIR data (Fig. 10A). We can construct a synchronous correlation square, by connecting the two autopeaks and the two cross-peaks (Fig. 10B), implying that a correlation exists between the two NIR bands at 4800 and 5200 cm^{-1} [32–36].

We may interpret these correlation peaks on the basis of the time-resolved NIR results. As discussed previously the time dependence of the NIR bands in the 5100–5300 cm^{-1} region indicates the consumption of water molecules and silanols in the reaction, while that of the bands in the 4600–4900 cm^{-1} region obviously reflects an increase in the amount of ethanol released and enhancement of the $NH_2 \cdots OH$ interaction, as a consequence of the ethanol release. Accordingly, we may assume that a strong autocorrelation peak reflects the time-dependent consumption of water molecules and silanols, while the two negative cross-peaks reflect the

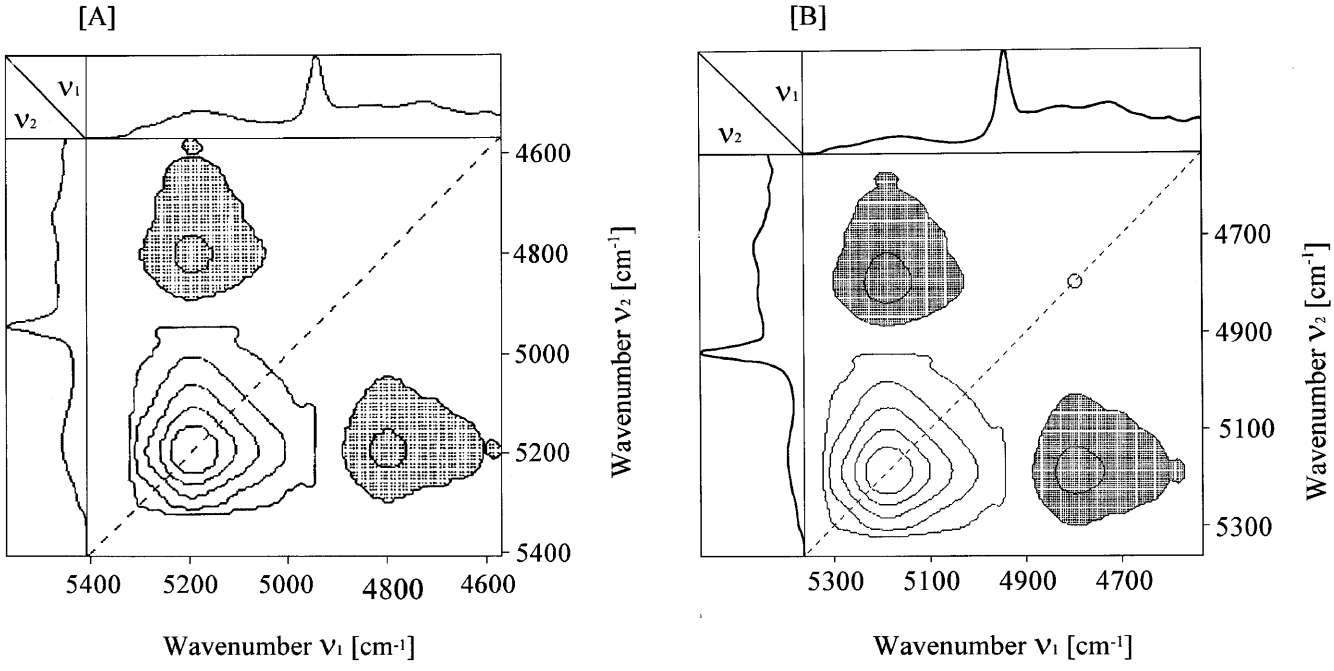

Fig. 10 Synchronous correlation spectra of the APTS–ethanol–water system (**A** calculated from the initial 2 h time-resolved NIR spectra and **B** calculated from the later 6 h time-resolved NIR spectra)

time-dependent extent of ethanol release and the increased $NH_2\cdots OH$ interaction [32–36].

The contour map of the asynchronous 2D NIR correlation spectra of the APTS–ethanol–water system is shown in Fig. 11. The asynchronous contour map (Fig. 11A) was calculated from the initial 2 h time-resolved spectra and the asynchronous map (Fig. 11B) from the later 6 h time-resolved data. In map A, the key-type cross-peak A is due to the NIR bands at 5265 and 5300 cm^{-1}, which derive from the ($\nu + 2\delta$) combination modes of strongly and weakly associated SiOH groups,

Fig. 11 Asynchronous correlation spectra of the APTS–ethanol–water system (**A** calculated from the initial 2 h time-resolved NIR spectra and **B** calculated from the later 6-h time-resolved NIR spectra) [*A*(5295, 5214), *B*(5190, 5140), *C*(5164, 4950), *D*(5190, 4920), *E*(5190, 4730), *F*(4955, 4755), *A′*(5300, 5260), *B′*(5190, 5140), *C′*(5146, 4955), *D′*(5180, 4927), *E′*(5200, 4730), *F′*(4955, 4755), *G′*(4930, 4775)]

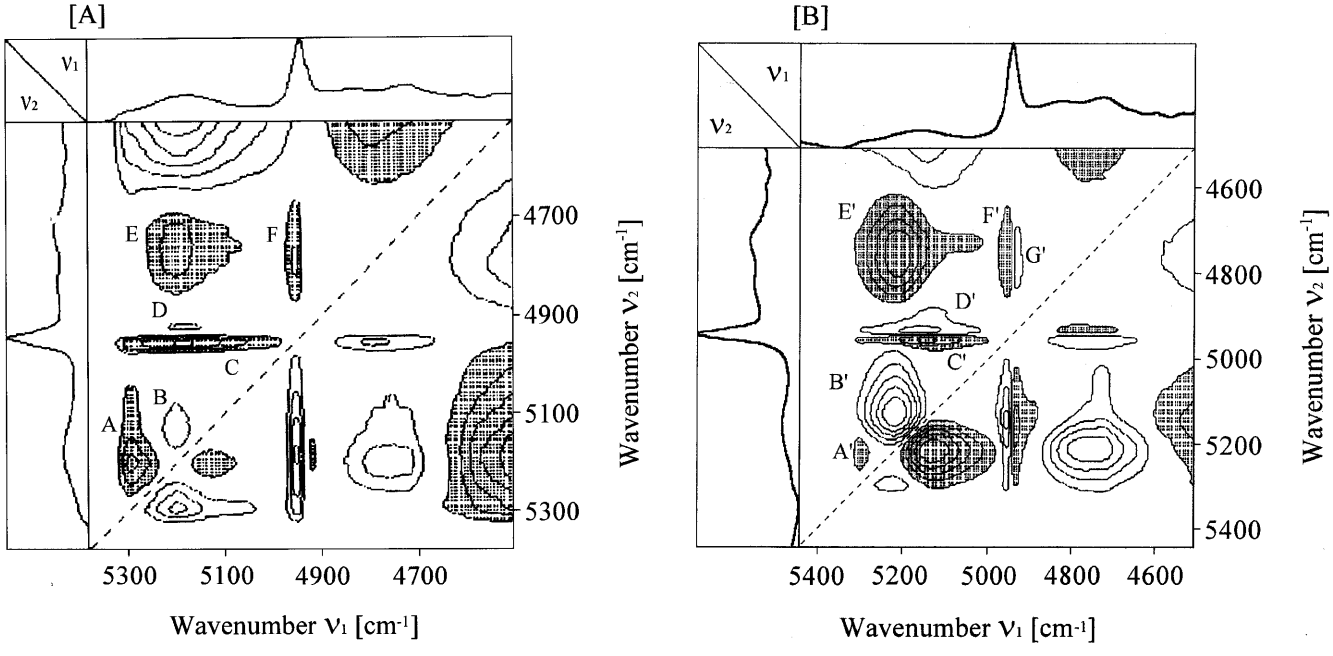

respectively, i.e. superimposition of the rodlike cross-peak at coordinate (5300, 5050–5200) and the cross-peak at coordinate (5265, 5190), which have similar trends in intensity variation, gives rise to this key-type cross-peak A. The negative sign of cross-peak A implies that the variation in intensity of the water ($\nu_2 + \nu_3$) combination bands at 5050–5200 cm^{-1} occurs faster than that of the 5265 and 5300 cm^{-1} bands, indicating that consumption of water molecules occurs more rapidly than that of the SiOH groups.

The positive and weak cross-peak B is due to the NIR bands at 5189 and 5140 cm^{-1} arising from the ($\nu_2 + \nu_3$) combination bands of water molecules in different hydrogen-bonding environments. The positive sign of this cross-peak reveals that the intensity variation (decrease) of the 5140 cm^{-1} band occurs more slowly than that of the 5189 cm^{-1} band. Therefore, we may assume that consumption of water molecules, which participate in the weak hydrogen-bonding system, in the hydrolysis reaction occurs faster than that of strongly hydrogen bonded water molecules.

It is evident that the rodlike, strong cross-peak C indicates a correlation (probably through hydrogen bonding) between the broad silanol ($\nu + 2\delta$) and water combination ($\nu_2 + \nu_3$) bands developed at 5000–5300 cm^{-1} and the 4950 cm^{-1} band arising from the [$\nu_{asy}(NH_2) + \delta(NH_2)$] combination modes. The negative sign of this rodlike cross-peak shows that the intensity variation of the 4950 cm^{-1} band occurs more rapidly than that of bands in the 5000–5300 cm^{-1} region.

The positive cross-peak D, which appeared as a consequence of enhancement of the spectral resolution, probably comes from the [$\nu_{asy}(NH_2) + \delta(NH_2)$] combination modes of NH_2 groups hydrogen-bonded weakly with water molecules, and indicates the correlation through a weak hydrogen-bonding network between the water 5189 cm^{-1} band and the NH_2 combination band at 4920 cm^{-1}. The temporal relationship between the 5189 and 4920 cm^{-1} bands cannot be determined from the positive sign of the cross-peak, since the synchronous correlation intensity at the same coordinate is zero (Fig. 10A).

The negative cross-peak E mainly comes from correlation between the water ($\nu_2 + \nu_3$) combination bands and the ethanol 4802 cm^{-1} band or the [$\nu_{asy}(NH_2) + \delta(NH_2)$] combination bands of NH_2 groups participating in a relatively strong hydrogen-bonding network. The negative sign of this cross-peak shows that the intensity variation of the water ($\nu_2 + \nu_3$) bands at 5190 cm^{-1} occurs more rapidly than that of either the NH_2 combination band at 4950 cm^{-1} or the ethanol 4802 cm^{-1} band. The other rodlike, negative cross-peak F indicates a correlation between the 4950 cm^{-1} band arising from the NH_2 combination modes and the ethanol 4802 cm^{-1} band. We cannot determine the temporal relationship between the two bands, since the synchronous correlation intensity at the same coordinate vanishes (Fig. 10A).

In contour map B, which was calculated from the later 6 h time-resolved data, it is found that a marked variation in the features of the cross-peaks occurs. The negative and weak cross-peak A′, arising from the 5300 cm^{-1} band for the weakly associated SiOH groups, does not involve a contribution from the component band at 5265 cm^{-1}. Therefore, an intensity variation (that is, decrease) in only the 5300 cm^{-1} band for the weakly associated SiOH groups mainly occurs in the later step, implying that the intensity variation of the 5265 cm^{-1} band for the strongly associated SiOH groups does not occur in this step, reflecting the result of the kinetics analysis for the 5265 cm^{-1} band, as discussed earlier. In other words, consumption of the strongly associated silanol groups is almost finished in the initial 2 h, while the weakly associated silanols are utilized for the condensation reaction over the whole reaction time. The negative sign of cross-peak A′ implies that consumption of strongly associated SiOH groups occurs faster than that of weakly associated SiOH groups.

The presence of the positive and very strong cross-peak B′, which comes from the 5189 cm^{-1} band of water molecules, implies that the intensity decrease of the 5189 cm^{-1} band predominantly occurs in the later step and that this variation occurs faster than that of the 5140 cm^{-1} band of the water molecules participating in the strong hydrogen-bonding network. This fact indicates that the consumption of water molecules participating in a weak hydrogen-bonding system occurs more rapidly than that of those in the strong hydrogen-bonding system.

We note that the intensity of cross-peak D′ is stronger than that of cross-peak D in map A, implying an increase in the number of NH_2 groups hydrogen-bonded weakly with water molecules in the later step rather than in the initial step.

When we compare map B with map A, we note that the contour level of cross-peak E′, corresponding to cross-peak E in map A, is extended toward $\nu_1 = 5000$ cm^{-1} on the line of $\nu_2 = 4730$ cm^{-1} in the later step, showing the existence of a correlation between the silanol and water OH bands and the 4730 cm^{-1} band. This fact implies that a strong interaction through hydrogen bonding between these OH and NH_2 groups occurs in the later step, cross-peak G′, in which the corresponding cross-peak is absent in map A, appears as a consequence of resolution enhancement, revealing the appearance of the correlation through weak hydrogen bonding between the 4930 cm^{-1} band and the ethanol 4802 cm^{-1} band in the later step. We cannot determining the temporal relationship between the two bands, providing cross-peak G′, for the same reason (Fig. 10B).

Thus, there exists a marked difference between asynchronous maps A and B, which reflects the

microstructural variation in the initial and second steps for the APTS–ethanol–water reaction system.

Conclusion

The time-resolved NIR spectra of the APTS–ethanol–water system were measured and deconvolution of these spectra was carried out. The existence of component bands at 5189, 5265 and 5300 cm^{-1} was confirmed in the 5000–5400 cm^{-1} region. The band at 5189 cm^{-1} was assigned to the so-called ($\nu_2 + \nu_3$) combination mode of an H_2O molecule. The bands at 5265 and 5300 cm^{-1} were assigned to the combination ($\nu_{SiOH} + 2\delta$) mode of the OH stretch (ν_{SiOH}) and bend (δ) modes, respectively, of the SiOH groups. The former band may be due to strongly associated and the latter band to weakly associated silanols. The integral intensities of these three component bands, which decrease markedly with reacted time, were utilized to discuss the kinetics of the hydrolysis and condensation reactions.

In particular, the time-dependent downward shift of the 5189 cm^{-1} band obviously reflects the variation in the environment of water molecules during the polymerization process. In the initial step, water molecules probably participate in the relatively weak hydrogen-bonding system formed by small oligomeric clusters, including dimers and trimers, while in the second step, water molecules may be incorporated into the stronger hydrogen-bonding system formed by polymeric clusters. Therefore, we may assume that water molecules in such a restricted state affect the rate of the hydrolysis and condensation reactions.

The polymerization process is reflected in the 2D NIR correlation spectra. Especially, in the asynchronous 2D NIR correlation spectra, the features in the contour maps are strongly dependent upon reaction time and the difference in the feature between maps A and B obviously reflects the dynamic behavior of silanols, water and ethanol molecules in the reaction process. We conclude that 2D correlation spectra serve as a powerful tool for following such reactions.

Acknowledgement We wish to thank K. Ozaki, Department of Chemistry, School of Science, Kwansei Gakuin University, for his generous offer of the program 2D-Pocha for generalized 2D correlation spectroscopy.

References

1. Johannson OK, Stark FO, Vogel GE, Fleishmann RM (1967) J Compos Mater 1:278
2. Lee LH (1968) J Colloid Interface Sci 27:751
3. Schrader ME (1970) J Adhes 2:202
4. Bascom WD (1972) Macromolecules 5:792
5. Shih PTK, Koenig JL (1975) Mater Sci Eng 20:145
6. (a) Batuev MI, Shostakovskii MF, Belyaev VI, Matvecva AD, Dubrova EW (1954) Dokl Akad Nauk SSSR 95:531; (b) Chem Abstr (1955) 49:6089
7. Benesi HA, Jones AC (1959) J Phys Chem 63:179
8. Richards RE, Thompson HW (1949) J Chem Soc 124
9. Chiang C-H, Ishida H, Koenig JL (1980) J Colloid Interface Sci 74:396
10. Murthy RSS, Leyden DE (1986) Anal Chem 58:1228
11. Murthy RSS, Biltz JP, Leyden DE (1986) Anal Chem 58:3167
12. McKenzie MT, Culler SR, Koenig JL (1984) Appl Spectrosc 38:786
13. Morral SW, Leyden DE (1985) In: Leyden DE (ed) Silanes, surface and interfaces. Gordon and Breach, New York, p 501
14. Vrancken KC, Van Der Voort P, Gillis-D'Hamers I, Vansant EF, Grobet P (1992) J Chem Soc Faraday Trans 88:3197
15. Vrancken KC, Coster LD, Van Der Voort P, Grobet PJ, Vansant EF (1995) J Colloid Interface Sci 170:71
16. Shimizu I, Yoshino A, Okabayashi H, Nishio E, O' Connor CJ (1997) J Chem Soc Faraday Trans 93:1971
17. Shimizu I, Okabayashi H, Taga K, O' Connor CJ (1997) Colloid Polym Sci 275:555
18. Yoshino A, Okabayashi H, Shimizu I, O'Connor CJ (1997) Colloid Polym Sci 275:672
19. Okabayashi H, Shimizu I, Nishio E, O' Connor CJ (1997) Colloid Polym Sci 275:744
20. Shimizu I, Okabayashi H, Taga K, Nishio E, O'Connor CJ (1997) Vib Spectrosc 14:113
21. Shimizu I, Okabayashi H, Taga K, Yoshino A, Nishio E, O'Connor CJ (1997) Vib Spectrosc 14:125
22. Plueddemann EP (1974) In: Brautman LJ, Krock RH (eds) Interface in polymer matrix composites in a series of composite materials, vol 6. Academic New York, p1
23. Boerio FJ, Shoenlein LH, Greivenkamp JE (1978) J Appl Polym Sci 22:203
24. Anderson HR, Jr Fowkes FM, Hidelscher FH (1976) J Poly Sci Phys 14:879
25. Moses PR, Wier LM, Lennox JC, Finklea HO, Lenhard JR, Murrary RW (1978) Anal Chem 50:576
26. Ishida H, Chiang CH, Koenig JL (1982) Polymers 23:251
27. Child MJ, Heywood MJ, Pulton SK, Vicary GA, Yong GH, Rochester CH (1982) J Colloid Interface Sci 89:202
28. Zhdanov SP, Kosheleva LS, Titova TI (1987) Langmuir 3:960
29. Tripp CP, Hair ML (1993) J Phys Chem 97:5693
30. Morimoto T, Imai J, Nagao M (1974) J Phys Chem 78:704
31. Shimizu I, Okabayashi H, Hattori N, Taga K, Yoshino A, O'Connor CJ (1997) Colloid Polym Sci 275:293
32. Noda I (1986) Bull Am Phys Soc 31:520
33. Noda I (1989) J Am Chem Soc 111:8116
34. Noda I (1990) Appl Chem Soc 44:550
35. Noda I (1993) Appl Spectrosc 47: 1329
36. Ozaki Y, Liu Y, Noda I (1997) Appl Spectrosc 51:526
37. Ozaki Y, Noda I (1996) J Near-Infrared Spectrosc 4:85
38. Marcott C, Noda I, Dowrey AE (1991) Anal Chem Acta 250:131
39. Reynolds N (1991) Adv Mater 3:614
40. Gregorius VG, Chao JL, Tariumi H, Palmer RA (1991) Chem Phys Lett 179:491
41. Palmer RA, Manning CJ, Chao JL, Noda I, Dowrey AE, Marcott C (1991) Appl Spectrosc 45:12

42. Noda I, Dowrey AE, Marcott C (1993) 47:1317
43. Noda I, Liu Y, Ozaki Y (1996) J Phys Chem 100:8665
44. Noda I, Liu Y, Ozaki Y (1996) J Phys Chem 100:8674
45. Ozaki Y, Liu Y, Noda I (1996) 30:2391
46. Nabet A, Pezolet M (1997) Appl Spectrosc 51:466
47. Noda I, Liu Y, Ozaki Y, Czarnecki MA (1995) J Phys Chem 99:3068
48. Liu Y, Ozaki Y, Noda I (1996) J Phys Chem 100:7326
49. Kato M, Taniguchi Y, Sawamura S, Suzuki K (1992) In: Maeno N, Endoh (eds) Physics and Chemistry of ice. Hokkaido University Press, Sapporo, p 83
50. Wilson RM, Miller TL (1975) Anal Chem 47:256
51. Nogami M, Morita Y (1979) Yogyo-Kyokai-Shi 87:43
52. Nishio E, Ikuta N, Okabayashi H, Hannah RW (1990) Appl Spectrosc 44:614
53. Ogasawara T, Izawa K, Hattori N, Okabayashi H, O'Connor CJ (1999) Colloid Polym Sci
54. Ogasawara T, Yoshino A, Okabayashi H, O'Connor CJ (1999) Colloids Surfaces 163:(in press)